Electric charge dequantization with Dirac neutrinos in CEνNS

Amir N. Khan[*]

Max-Planck-Institut für Kernphysik, Postfach 103980, D-69029 Heidelberg, Germany

(Dated: February 24, 2022)

Observation of electrically charged neutrinos is crucial for charge dequantizaton and for revealing the nature of the neutrino. We analyze new data of the COHERENT experiment for the coherent neutrino-nucleus scattering to investigate the electric charges of neutrinos. With almost double the statistics and precision now, the statistical significance of the observed process has been enhanced to 11.6σ. We show how the sensitivity or limits of the neutrino electric charges depend differently on the interference effect, inverse power of recoil energy and on the mass of the target particle than the other electromagnetic properties. We derive constraints all electromagnetic properties of neutrinos using the new COHERENT data.

PACS numbers: xxxxx

I. INTRODUCTION

The origin of the experimental observation that electric charge is quantized in nature is not predicted but rather assumed in the Standard Model (SM). However, several theories beyond the SM like those with magnetic monopoles [1], grand unified theories [2, 3] and the extra dimension models [4] do predict the charge quantization. In addition, there are several extensions of the SM that predict new particles with fractional charges [5–9]. The fractionally charged particles are also promising candidates for dark matter [10–17]. Even charges of the SM particles can deviate from the integer multiple of 'e/3', where 'e' is the magnitude of unit electric charge. Neutrinos are the favorite candidates for such particles, often called milli-charged neutrinos [18–21].

The SM is an anomaly-free gauge theory with several accidental global symmetries. In the SM with one generation of fermions, neutrinos are exactly neutral because all the SM anomalies consistently cancel out. However, for the SM with three generations, at least two of the three massless neutrinos could be electrically charged. This dequantization leads to the emergence of three gaugeable $U(1)$ symmetries, $L_e - L_\mu$, $L_\mu - L_e$ and $L_e - L_\tau$. Only one of the three differences can be anomaly-free and the corresponding difference is added to the hypercharge of the SM which leads to the fractional charges of neutrinos and thus the dequantization of electric charge at least in the lepton sector [20, 21].

For massive neutrinos, the existence of fractional charges of neutrinos depends on the nature of their masses. If neutrinos are Majorana fermions, then new anomalies arise but they cancel

---

out, leaving neutrinos as neutral [18, 19]. Consequently, the electric charge still remains quantized in the minimally extended SM. On the other hand, Dirac neutrinos with three right-handed partners, singlets under $SU(3)_c \times SU(2)_L$, are electrically charged. This also modifies the charges of the charged leptons and quarks due to the consistent dependence of their hypercharges on the hypercharge of the right-handed neutrinos. This leads to the dequantization of electric charges in general [20, 21]. This dequantization is related to the emergence of anomaly-free gaugeable $B - L$ symmetry [18]. From the theoretical considerations, there is no upper limit available on the millicharge neutrinos. All the known limits are experimental [22–31] or observational [32–36].

We analyze the new data of coherent elastic neutrino-nucleus scattering (CEνNS) from the COHERENT experiment for sensitivities of the neutrinos millicharges. CEνNS is a SM process observed by the COHERENT experiment [37, 38] and was predicted forty years ago [39–42]. The importance of the process ranges from its ability to probe SM parameters [39–48] and test new interactions at low momentum transfer [49–59]. The collaboration has updated the result for the observed process by doubling the statistics and the precision by reducing the overall systematic errors to half [60]. In particular, the error in the quenching factor has been improved from 25% to 4%. Compared to the first result at 6.7σ, the updated significance level has now reached 11.6σ. With this improvement, it is natural to expect a better sensitivity to any new physics or improvements in the limits.

In low energy scattering experiments with low target recoils, the sensitivity to any new physics mainly depends on three factors: (i) whether the new physics interactions interfere with the SM interactions or not, (ii) what inverse power of the target recoiled energy enters into the proportionality of new physics interactions and (iii) size of the target particle mass. Among the various nonstandard neutrino interactions, the fractionally charged neutrino is the most sensitive candidate at low energy recoils [31, 61, 62], because they interfere with the SM interactions and their couplings are proportional to the square of the target recoil energy. We will focus on these aspects in this work. Note that these kinematical considerations are equally valid for the target recoils in the dark matter scattering [63]. In addition we will derive constraints on all electromagnetic properties of neutrinos using the new COHERENT data.

The paper is organized as follows. In the next section, we discuss the basics of the differential cross-section of the CEνNS in the SM. In Sec. III, we discuss data analysis for the COHERENT set up with the new data. In Sec. IV, we introduce the electromagnetic properties of neutrinos and derive constraints using the new COHERENT data. In Sec. V, we discuss in detail that why millicharge neutrinos have kinematically special than the other electromagnetic properties of neutrinos. Finally, we provide conclusion of this work in sec VI.

II.   COHERENT ELASTIC NEUTRINO NUCLEUS SCATTERING

At the tree level in SM, the differential cross-section of the neutrino with flavor 'α' scattering off the spin-0 nucleus of CsI with proton number 'Z' and neutron number 'N' is given by [39–44],

$$\frac{d\sigma_\alpha}{dT}(E_\nu, T) = \frac{G_F^2 M}{\pi} \left[Z g_p^V + N g_n^V) \right]^2 \left(1 - \frac{T}{E_\nu} - \frac{MT}{2E_\nu^2} \right) F^2(q^2), \tag{1}$$

where 'G_F' is the Fermi constant, 'E_ν' is the energy of the incoming neutrinos, 'T' is nuclear recoil energy, $q^2 = 2MT$ is the squared momentum transfer, 'M' is the mass of the target nucleus. Here, $g_p^V = (2g_u^V + g_d^V)$ and $g_n^V = (g_u^V + 2g_d^V)$, where g_u^V and g_d^V are the neutral current coupling constants for the 'up' and 'down' quarks which, in terms of the weak mixing angle 'θ_W' are given by

$$g_u^V = \frac{1}{2} - \frac{4}{3} \sin^2 \theta_W, \tag{2}$$

$$g_d^V = -\frac{1}{2} + \frac{2}{3} \sin^2 \theta_W. \tag{3}$$

To include all the radiative corrections, we will use $\sin^2\theta_W = 0.23857 \pm 0.00005$, the low energy value evaluated in $\overline{\text{MS}}$ scheme [64–66]. In Eq. (1), $F(q^2)$ is nuclear form factor, where we use the Klein-Nystrand form factor [67] as given in the following

$$F(q^2) = \frac{4\pi\rho_0}{Aq^3} [\sin(qR_A) - qR_A \cos(qR_A)] \left[\frac{1}{1 + a^2 q^2} \right], \tag{4}$$

where ρ_0 is the normalized nuclear number density, A is the atomic number of CsI, $R_A = 1.2A^{1/3}$ fm is the nuclear radius, and $a = 0.7$ fm is the range of the Yukawa potential.

III.   DATA ANALYSIS

The COHERENT detector receives a prompt signal of mono-energetic (29.8 MeV) beam of muon-neutrinos (ν_μ) produced from the π^+ decay at rest ($\pi^+ \to \mu^+ \nu_\mu$) at Oak Ridge Spallation Neutron Source. Subsequently, a continuous flux of electron-neutrinos (ν_e) and muon-anti-neutrinos ($\bar{\nu}_\mu$) with energy peaks, respectively, around 35 Mev and 52.8 MeV produced in μ^+ decays ($\mu^+ \to \nu_e e^+ \bar{\nu}_\mu$) with a time of delay of 8.5 μs, are received. The fluxes are produced from 3.20×10^{23} protons on target from the liquid mercury. The average production rate of the SNS neutrinos from the pion decay chain is $r = 0.0848$ neutrinos of each flavor per proton [60].

The detector at a distance $L = 19.3$ m from the source uses CsI[Na] as a target, where the Na contributes small enough to be neglected. For such a setup, the total number of events of the nuclear recoil in a given energy bin 'i' and neutrino flavor 'α' reads

$$N_\alpha^i = N \int_{T'^i}^{T'^{i+1}} dT' \int_0^{T^{\max}} dT \int_{E_\nu^{\min}}^{E_\nu^{\max}} dE_\nu \frac{d\sigma_\alpha}{dT}(E_\nu, T) \frac{d\phi_{\nu_\alpha}(E_\nu)}{dE_\nu} \mathcal{E}(T') G(T', T), \tag{5}$$

where $\mathcal{E}(T')$ is the detection efficiency function, $G(T', T)$ is the gamma distribution function for the detector energy resolution, T and T' denote respectively the nuclear recoil energy and the reconstructed recoil energy. Both $\mathcal{E}(T')$ and $G(T', T)$ were taken from ref. [60]. Here, $N = (2m_{\text{det}}/M_{\text{CsI}})\,N_A$ is the total number of CsI nucleons, $m_{\text{det}} = 14.57$ kg, N_A is the Avogadro's number, M_{CsI} is the molar mass of CsI, $E_\nu^{\text{min}} = \sqrt{MT/2}$, M is the mass of the target nucleus, E_ν^{max} is the maximum neutrino energy and $d\phi_{\nu_\alpha}(E_\nu)/dE_\nu$ is the flux corresponding to the flavor 'α' [58].

The recent measurement of COHERENT [60] considers the recoiled energy-dependent quenching factor, $f_q(T')$ and measures the energy spectrum in terms of photo-electrons (p.e). Therefore, to calculate the total number of events in a particular bin 'i' of photo-electrons, we use the following relation between the recoil energy and the number of photo-electrons ($N_{\text{p.e}}$)

$$N_{\text{p.e.}} = f_q(T') \times T' \times Y, \tag{6}$$

where Y = 13.35 photons/keV is the light yield and $f_q(T')$ is taken from [60].

To fit data of the energy spectrum in Fig. 3 of ref. [60] with the model including the SM and the neutrino electric charge parameters, we use the following least-square function

$$\chi^2 = \sum_{i=2}^{9} \left(\frac{N_{\text{obs}}^i - N_{\text{exp}}^i(1+\alpha) - B^i(1+\beta)}{\sigma^i} \right)^2 + \left(\frac{\alpha}{\sigma_\alpha} \right)^2 + \left(\frac{\beta}{\sigma_\beta} \right)^2, \tag{7}$$

where N_{obs}^i denotes the observed events above the steady-state background in the i-th energy bin and σ^i is the relevant uncertainty [60], N_{exp}^i is the total expected events as a sum of the three neutrino flavors as given in eq. (5) and B^i is the sum of prior predicted beam-related neutron and the neutrino-induced neutron backgrounds in the given energy bin. The first and second penalty terms respectively correspond to the systematic uncertainty related to the signal and backgrounds where 'α' and 'β' are the corresponding nuisance parameters. The uncertainty in the signal is σ_α = 0.127 and the uncertainty in the total background is $\sigma_\beta = 0.6$. The signal uncertainty includes a contribution from the neutrino flux, quenching factor, efficiency, form factor and the light yield. All information was taken from ref. [60]. Notice the timing information between the prompt and delayed signal are there but small and therefore we do not include them in our analysis [60]. In this regard, we consider our results to be conservative. Stronger constraints are expected when the timing information is also included. The only parameter that is affected by the timing information is the total efficiency. However, since the energy-dependent and the small time-dependent efficiencies are uncorrelated [60], and the results are not affected by this subtlety.

IV.   ELECTROMAGNETIC INTERACTIONS OF NEUTRINOS IN CEνNS

A.   Millicharge neutrinos

The electromagnetic contribution due to the electrically charged neutrinos, parameterized in terms of $Q_{\alpha\alpha}$, to the SM weak interaction for the coherent neutrino-nucleus ($\nu - N$) scattering is given by the interactions

$$\mathcal{L}_\alpha^{em} = -ie \left(Q_{\alpha\alpha} \overline{\nu}_\alpha \gamma_\mu \nu_\alpha + \overline{N} \gamma_\mu N \right) A^\mu, \tag{8}$$

where A^μ is mediating electromagnetic field and 'e' is the unit electric charge. Since the electromagnetic interaction terms adds coherently to the vector part of the weak interaction, this modifies the weak mixing angle θ_W in eq. (3) accordingly as

$$\sin^2 \theta_W \to \sin^2 \theta_W \left(1 - \frac{\pi \alpha_{em}}{\sqrt{2} \sin^2 \theta_W G_F MT} Q_{\alpha\alpha} \right) \tag{9}$$

where α_{em} is the fine structure constant.

We estimate the statistical significance of the millicharge neutrinos by fitting the two parameters, Q_{ee} and $Q_{\mu\mu}$. We consider two cases while fitting parameters. First, we fit one parameter at a time and fix the other to zero and the result is shown in the left-side plot of Fig. 1. Next, we fit the two parameters together and results are shown in the right-side plot of Fig. 1. As can been from Fig. 1 that because of the interplay between the SM and the neutrino millicharge contribution (interference effect) and the dependence on the inverse double power of the nuclear recoil energy in the cross section, the both one parameter and two parameter fits prefer a non-zero best fit values. We obtain the following constraints from the one parameter fits at 90% C.L.,

$$\boxed{\begin{aligned} -0.55 \times 10^{-7} &< Q_{\mu\mu}/e < 0.75 \times 10^{-7}, \\ -1.10 \times 10^{-7} &< Q_{ee}/e < 3.90 \times 10^{-7}. \end{aligned}} \tag{10}$$

Stronger limits on millicharge neutrinos come from the observational studies [32–36]. The strongest upper limit on the millicharge neutrino is $Q_\nu \leq 2 \times 10^{-15} e$ from the time arrival dispersion and the energy spread of neutrinos from SN1987A [32]. The laboratory bounds from the $\nu - e$ are also several orders of magnitude smaller in size than the bounds of this study [22–31]. For instance, the TEXONO experiment derives the limit, $Q_\nu \leq 2.1 \times 10^{-12} e$. However, this difference can be easily understood from the kinematical considerations as we will discuss in Sec. V. However, robustness of the bounds totally depends on the experimental details. It would be interesting to explore how the observational constraints also depend on the kinematical details of the astrophysical environments.
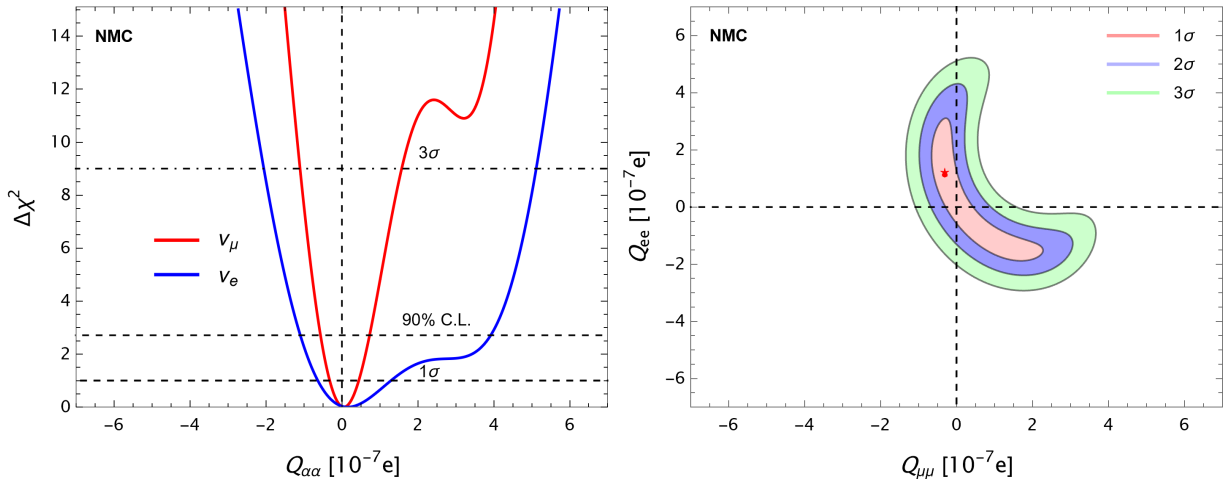
Fig. 1. Neutrino millicharge (NMC) of the muon and electron flavors from the new COHERENT data for one (left) and two (right) parameter fits. The red star in the right-hand side plot corresponds to the best-fit value. See text for discussion.
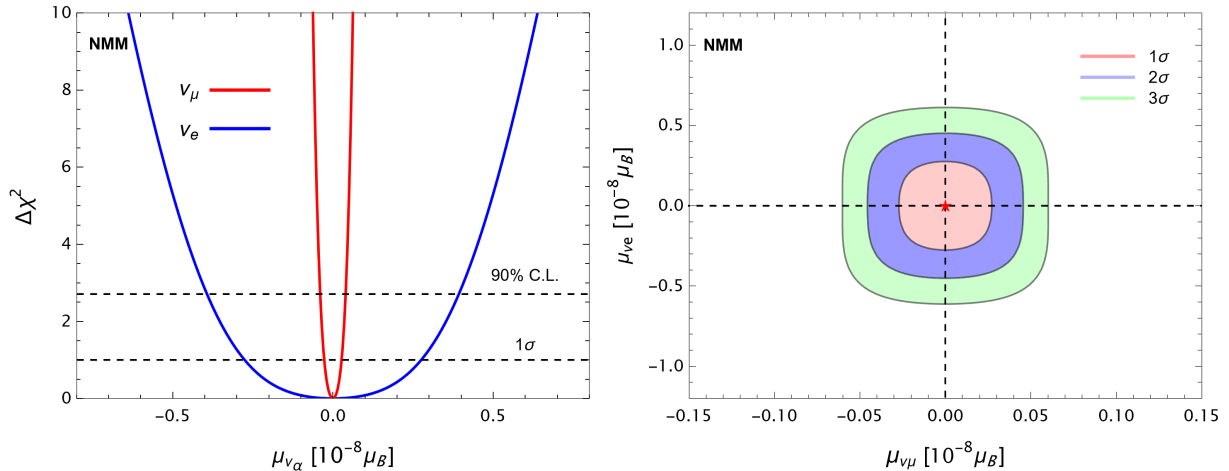
B. Neutrino magnetic moment

To understand the importance of interference and the low recoil energy dependence of the millicharge neutrinos we also fit the neutrino magnetic moment to the same data for comparison. In the general of coupling for Majorana (M) or Dirac (D) neutrinos to the electromagnetic field strength ($F^{\mu\nu}$) the magnetic moments appears as [68–71]

$$\mathcal{L}^M = -\frac{1}{4}\bar{\nu}^c_{\alpha L}\,\lambda^M_{\alpha\beta}\,\sigma_{\mu\nu}\,\nu_{\beta L}\,F^{\mu\nu} \quad \text{or} \quad \mathcal{L}^D = -\frac{1}{2}\bar{\nu}_{\alpha R}\,\lambda^D_{\alpha\beta}\,\sigma_{\mu\nu}\,\nu_{\beta L}\,F^{\mu\nu}\,, \tag{11}$$

where $\lambda^X = \mu^X - i\epsilon^X$, which is hermitian for the Dirac neutrinos and antisymmetric for Majorana neutrinos. For Majorana neutrinos, only transition magnetic moments are possible while the flavor diagonal are zero. Because of the unknown final state neutrino flavor in a scattering process, in practice no distinction between Dirac and Majorana neutrinos is possible. For simplicity, we only consider the flavor diagonal cases for electron ($\mu_{\nu e}$) and muon neutrinos ($\mu_{\nu\mu}$). In the SM, non-zero neutrino magnetic moment can arise at one-loop level which is quantified as [68, 69]

$$\mu_{\alpha\beta} = \frac{3eG_F m_\nu}{8\sqrt{2}\pi^2} \sim 3 \times 10^{-19}\mu_B\left(\frac{m_\nu}{1\text{eV}}\right) \tag{12}$$

As clear from eq. (11), the helicity of the final state neutrino changes in interaction due to magnetic moment, therefore there is no interference with the SM cross-section and the corresponding contribution adds to the standard model at the cross-section level. We add the following differential cross-section [28] for the neutrino magnetic moment (MM) of neutrino scattering off a spin-0

Fig. 2. Neutrino magnetic moment (NMM) of the electron and muon neutrino from the new COHERENT data for the one (left) and two (right) parameters fits. The red star in the right-hand side plot corresponds to the best-fit value. See text for discussion.

nuclei to the SM cross-section in eq. (1),

$$\frac{d\sigma_\alpha^{MM}}{dT}(E_\nu, T) = \left(\frac{\pi\alpha_{em}^2\mu_{\nu\alpha}^2}{m_e^2}\right) \left(\frac{1}{T} - \frac{1}{E_\nu} + \frac{T}{4E_\nu^2}\right) Z^2 F^2(q^2),$$ (13)

where the magnetic moment ($\mu_{\nu\alpha}$) is given units of Bohr's magneton (μ_B) and m_e is the electron mass. One can notice that in comparison to the millicharge of neutrinos as given in eq. (9) in combination with eq. (1), the neutrino magnetic moment has no interference with the SM and the dependence on the inverse power of the nuclear recoil is only linear in the leading terms.

In this case we consider two parameters μ_{ν_μ} and μ_{ν_e} and fit them to the new COHERENT data [60] using eq. (7), first, with one parameter at a time while keeping the other zero and then fit two parameters together. The results for both cases are shown respectively in the left-side and right-side plots of Fig. 2. We obtain the following constraints from the one-parameter fits at 90% C.L.,

$$-0.04 \times 10^{-8} < \mu_{\nu_\mu}/\mu_B < 0.04 \times 10^{-8},$$
$$-0.40 \times 10^{-8} < \mu_{\nu_e}/\mu_B < 0.40 \times 10^{-8}.$$ (14)

C.   Neutrino charge radius

In the SM neutrino charge radius for neutrinos is induced by radiative corrections. In the general effective electromagnetic vertex of massive neutrinos, $\bar{\nu}\Lambda_\mu\nu A^\mu$, the neutrino charge radius

term is given by [72–74],

$$\Lambda_\mu(q) = \gamma_\mu F(q^2) \simeq \gamma_\mu q^2 \frac{\langle r^2 \rangle}{6} , \tag{15}$$

where q is the momentum transfer and $F(q^2)$ is a form factor related to the neutrino charge radius $\langle r_\nu^2 \rangle$ via

$$\langle r_\nu^2 \rangle = 6 \left. \frac{dF_\nu(q^2)}{dq^2} \right|_{q^2=0} . \tag{16}$$

The SM prediction for the charge radius of neutrino [72–76] is

$$\langle r_{\nu_\alpha}^2 \rangle_{\text{SM}} = -\frac{G_F}{2\sqrt{2}\pi} \left[3 - 2 \ln \left(\frac{m_\alpha^2}{m_W^2} \right) \right] , \tag{17}$$

where m_α is the mass of the charged lepton associated to ν_α and m_W is the mass of the $W^\pm$ boson. The numerical values for the corresponding flavor of neutrinos are [72–76]

$$\langle r_{\nu_e}^2 \rangle_{\text{SM}} = -0.83 \times 10^{-32} \ \text{cm}^2,$$
$$\langle r_{\nu_\mu}^2 \rangle_{\text{SM}} = -0.48 \times 10^{-32} \ \text{cm}^2,$$
$$\langle r_{\nu_\tau}^2 \rangle_{\text{SM}} = -0.30 \times 10^{-32} \ \text{cm}^2. \tag{18}$$

In the SM, only flavor diagonal charge radii exist, while in general transition charge radii are also possible [76]. We consider here only the former case whose contribution add to SM cross-section coherently. This contribution can be added to the coherent cross-section by making the following replacement for the effective weak mixing angle in eq. (3),

$$\sin^2 \theta_W \rightarrow \sin^2 \theta_W \left(1 + \frac{\pi \alpha_{em}}{3\sqrt{2} \sin^2 \theta_W G_F} \langle r_{\nu_\alpha}^2 \rangle \right) \tag{19}$$

Notice that unlike the millicharge neutrinos in eq. 9, the charge radius is does not have a direct dependence on the nuclear recoil energy and the target mass and thus one cannot expect enhanced sensitivity at low energy recoils. This was also noted before in refs [31, 77]. We fit $\langle r_{\nu_e}^2 \rangle$ and $\langle r_{\nu_\mu}^2 \rangle$ with the new COHERENT data first by taking one parameter at a time and then the two parameters together. The obtained results are shown in Fig. 3 and constraints from one parameter-at-a-time at 90% C.L. are in the following

$$\boxed{\begin{aligned} -0.60 \times 10^{-30} < \langle r_{\nu_\mu}^2 \rangle / \text{cm}^2 < 0.05 \times 10^{-30}, \\ -0.67 \times 10^{-30} < \langle r_{\nu_e}^2 \rangle / \text{cm}^2 < 0.10 \times 10^{-30} . \end{aligned}} \tag{20}$$

D. Neutrino anapole moment

If neutrino carries a non-zero charge radius, it can also have a non-zero anapole moment [75, 78–84]. It determines the correlation between the spin and charge distributions of neutrinos and is defined in the same dimensions as that of the charge radius. In the general vertex for electromagnetic interactions, $\bar{\nu}\Lambda_\mu \nu A^\mu$, the anapole term is defined by [80, 81, 84]

$$\Lambda_\mu(q) = -\gamma_\mu \gamma_5 F(q^2) \simeq -\gamma_\mu \gamma_5 q^2 \boldsymbol{a}_\nu , \tag{21}$$

where the form factor '$F(q^2)$' is related to the neutrino anapole moment '$\boldsymbol{a}_{\nu_\alpha}$' by the expression,

$$\boldsymbol{a}_\nu = - \left. \frac{dF_\nu(q^2)}{dq^2} \right|_{q^2=0} . \tag{22}$$

By comparing with eq. (16), the SM prediction for the neutrino anapole moment can be written in terms of the charge radius as [75, 76, 80, 81, 84]

$$\boldsymbol{a}_{\nu_{\mathrm{SM}}} = -\frac{\langle r_\nu^2 \rangle_{\mathrm{SM}}}{6}, \tag{23}$$

and numerical values accordingly are,

$$\boldsymbol{a}_{\nu_{e\mathrm{SM}}} = 4.98 \times 10^{-32} \ \mathrm{cm}^2,$$
$$\boldsymbol{a}_{\nu_{\mu\mathrm{SM}}} = 2.88 \times 10^{-32} \ \mathrm{cm}^2,$$
$$\boldsymbol{a}_{\nu_{\tau\mathrm{SM}}} = 1.80 \times 10^{-32} \ \mathrm{cm}^2. \tag{24}$$

In case of the CEνNS, the contribution of the neutrino anapole moment can be added by replacing the effective weak mixing angle in eq. (3) as,

$$\sin^2 \theta_W \to \sin^2 \theta_W \left(1 - \frac{\pi \alpha_{em}}{18\sqrt{2}\sin^2 \theta_W G_F} \boldsymbol{a}_{\nu_\alpha} \right) \tag{25}$$

Again one can notice that unlike the neutrino millicharges, the anapole moment does not have a direct dependence on the nuclear recoil energy and the target mass and an enhanced sensitivity at low energy recoils is not expected. We fit the parameters $\boldsymbol{a}_{\nu_e}$ and $\boldsymbol{a}_{\nu_\mu}$ with the new COHERENT data. First, we fit one parameter at a time while fixing the other to zero and then fit the two parameters together. The obtained results are shown in Fig. 4 and constraints from this analysis in case of parameter-at-a-time at 90% C.L. are the following

$$\boxed{\begin{aligned} -0.30 \times 10^{-30} &< \boldsymbol{a}_{\nu_\mu}/\mathrm{cm}^2 < 3.7 \times 10^{-30} , \\ -0.60 \times 10^{-30} &< \boldsymbol{a}_{\nu_e}/\mathrm{cm}^2 < 4.0 \times 10^{-30} . \end{aligned}} \tag{26}$$
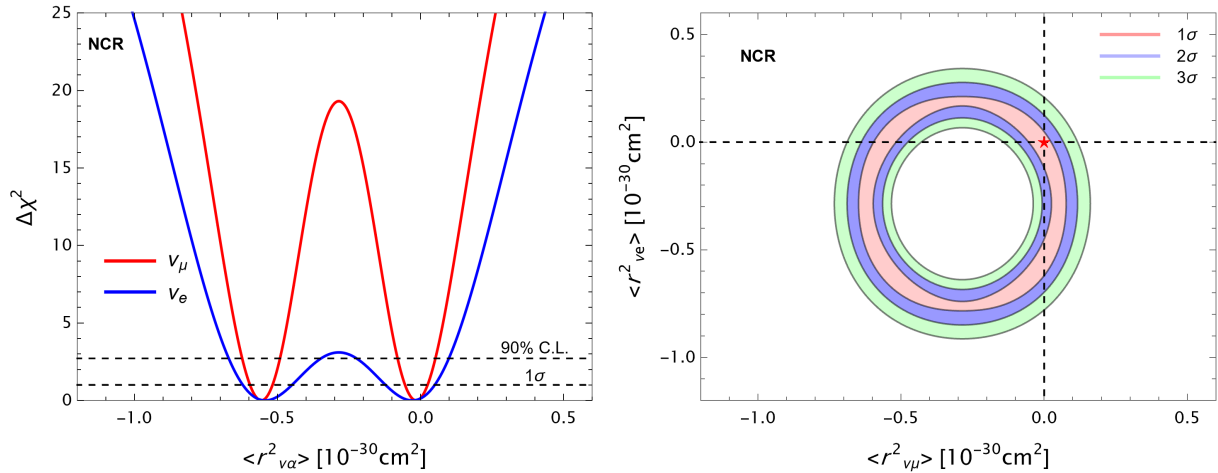
Fig. 3. Neutrino charge radius (NCR) of the electron and muon neutrino from the new COHERENT data for the one (left) and two (right) parameters fits. The red star in the right-hand side plot corresponds to the best-fit value. See text for discussion.
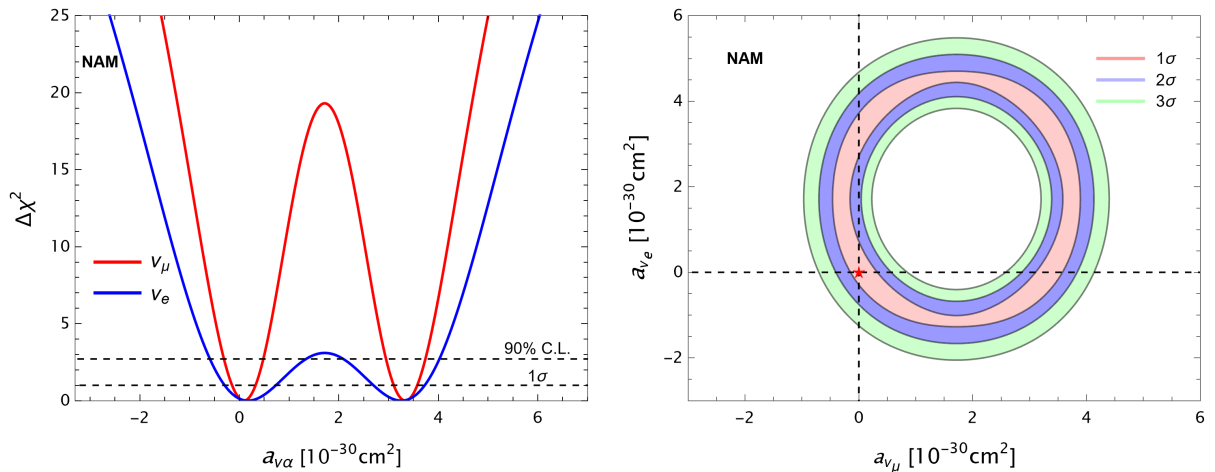
Fig. 4. Neutrino anapole moment (NAM) of the electron and muon neutrino from the new COHERENT data for the one (left) and two (right) parameters fits. The red star in the right-hand side plot corresponds to the best-fit value. See text for discussion.

V. WHY MILLICHARGE NEUTRINOS ARE EXPERIMENTALLY SPECIAL?

Neutrinos are electrically neutral in the SM. In several extensions of SM with Dirac neutrinos, the electric charges of the neutrino can arbitrarily take any values. Currently, all information about it comes from experiments. No theoretically predicted value is available. More importantly, the limits strongly depend on the process under consideration. There are three important factors that contribute to neutrino millicharges. These are the interference of their amplitude with the

standard model, inverse power dependence on the recoil energy and the size of the target mass. On the other hand, the other electromagnetic properties partially depend on these factors. For instance, there is interference of the neutrino charge radius and anapole moment with the SM but there is no inverse recoil energy and target mass dependence. For the neutrino magnetic moment, there is no interference with SM and no dependence on the target mass while there is only one power of inverse recoil energy dependence.

We show the millicharge dependence on the interference and on the inverse power of the recoil energy for the relevant fixed neutrino energy (30 MeV) and recoil energy (11 keV) in the left-hand side plots of Fig. 5. Here, the ratio between the new physics plus the SM differential cross-section and the SM alone cross-section for the four cases was taken as a function of the neutrino millicharge, magnetic moment, charge radius and anapole moment. In the region of interest for the CEνNS, the millicharge interactions compete with the SM cross-section up to $10^{-7}e$ and drops down to zero $3.3 \times 10^{-7}e$ at start starts growing afterwards, while the magnetic moment starts deviation from the SM at $10^{-9}\mu_B$, charge radius starts deviation from the SM at $10^{-31}cm^2$ and anapole moment starts deviation from the SM at around 10^{-31}cm^2.

To show the target mass dependence, we plot the second term of eq. (9) as a function of millicharge with target mass dependence, as given below,

$$f\left(Q\right) = \left(\frac{\pi\alpha_{em}}{\sqrt{2}\sin^2\theta_W G_F M T} Q_{\alpha\alpha} \right). \tag{27}$$

The comparison between a CsI nuclear target and any electronic target is shown in the right-hand side plot of Fig. 5. Clearly, the millicharge contribution is suppressed at $\mathcal{O}(10^3)$ due to the nuclear mass in comparison to electric recoils. At the cross-section level, this effect gets relatively weaker because the CEνNS cross-section is directly proportional to the target mass nucleus times the Z^2. However, the electronic targets still dominates and there is at least two orders of magnitude intrinsically stronger constraints on millicharge neutrinos in this case than the CEνNS. Notice that this property does not hold for the other three electromagnetic properties because of no inverse dependence on the target mass. Thus, the difference in the limits has a strong dependence on the difference between the electronic and the nuclear masses, no matter how different the precision of the two types of experiments is.

VI. CONCLUSIONS

Millicharge neutrinos are important from theoretical and observational points of view. Their observation would be strong evidence for physics beyond the SM and will have significant astrophysical implications. It will support the Dirac nature of neutrinos and the dequantization of the electric charges in the standard model. We have analyzed the new data of the CEνNS from the COHERENT experiment to search for the fractional electric charges of neutrinos and have shown
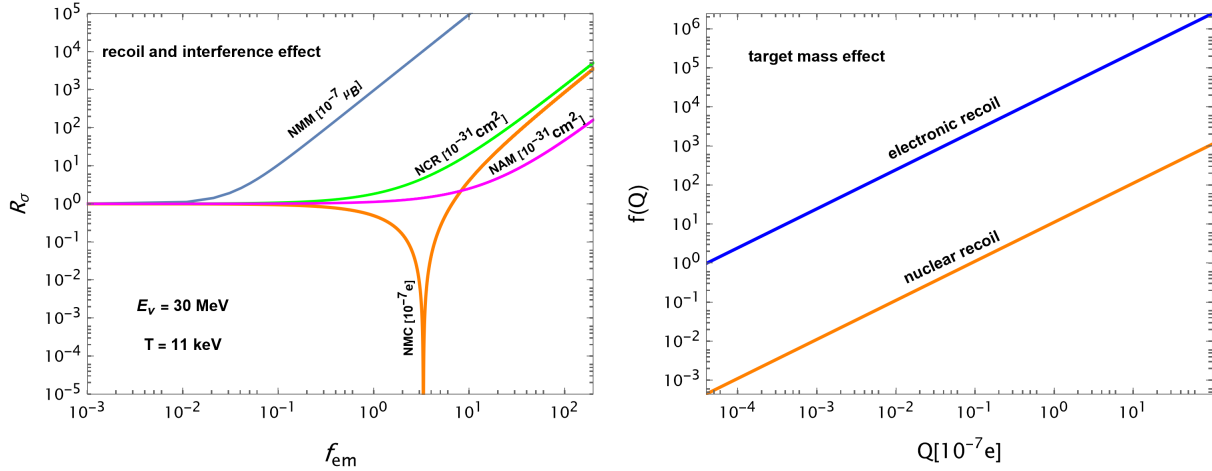
Fig. 5. Effects from interference and kinematics of the process. **Left** : The ratio between the millicharge, magnetic moment, charge radius and anapole moment plus the SM cross-sections and SM cross-section as a function of the millicharge, magnetic moment, charge radius and anapole moment at fixed neutrino energy and fixed nuclear recoil energy. **Right** : The millicharge term in Eq. 9 as a function of Q for the target nuclear and electronic masses. See text for the discussion.

their experimental sensitivity at low energy recoils in comparison to the neutrino magnetic moment, charge radius and anapole moment. By comparing the results in Figs. 1, 2, 3 and 4, it is clear that neutrino millicharges are relatively more sensitivity than the other electromagnetic properties of neutrinos because of their special kinematical behaviour. It is required to further investigate how the observational constraints depend on the kinematical details of the astrophysical environments.

We have shown that a better sensitivity of the millicharge neutrinos in comparison to the other nonstandard neutrino interactions is because of their enhanced dependence on the nuclear recoil and interference with standard model interactions while the sizes of constraints mainly depend on the size of the target particle mass. The rest is the experimental precision and statistics that matters for testing their sensitivity in an experiment. We have also shown that while their sizes depend on the specific interaction process, electronic targets can provide intrinsically stronger limits than the nuclear recoils. For completeness we have obtained stronger constraints on all electromagnetic properties using the latest data from the COHERENT experiment.

Note Added: In the first version of this work posted on arXiv, the addition of background in the predicted spectrum was missing which was leading to a statistically over-estimation of the sensitivity of neutrino millicharges. After including the background, the 3.5σ sensitivity reported in the first version now goes away, however, there is still a mild presence for neutrino millicharges in comparison to the other electromagnetic properties of neutrinos.

ACKNOWLEDGMENTS

---

[1] P. A. M. Dirac, Proc. Roy. Soc. Lond. A **133**, 60 (1931).

[2] H. Georgi and S. L. Glashow, Phys. Rev. Lett. **32**, 438 (1974).

[3] J. C. Pati and A. Salam, Phys. Rev. D **10**, 275 (1974), [Erratum: Phys.Rev.D 11, 703–703 (1975)].

[4] N. Arkani-Hamed, L. Motl, A. Nicolis, and C. Vafa, JHEP **06**, 060 (2007), arXiv:hep-th/0601001.

[5] A. Y. Ignatiev, V. A. Kuzmin, and M. E. Shaposhnikov, Phys. Lett. B **84**, 315 (1979).

[6] L. B. Okun, M. B. Voloshin, and V. I. Zakharov, Phys. Lett. B **138**, 115 (1984).

[7] B. Holdom, Phys. Lett. B **178**, 65 (1986).

[8] B. Batell and T. Gherghetta, Phys. Rev. D **73**, 045016 (2006), arXiv:hep-ph/0512356.

[9] K. Cheung and T.-C. Yuan, JHEP **03**, 120 (2007), arXiv:hep-ph/0701107.

[10] H. Goldberg and L. J. Hall, Phys. Lett. B **174**, 151 (1986).

[11] R. N. Mohapatra and I. Z. Rothstein, Phys. Lett. B **247**, 593 (1990).

[12] B. Kors and P. Nath, JHEP **07**, 069 (2005), arXiv:hep-ph/0503208.

[13] H. Gies, J. Jaeckel, and A. Ringwald, Phys. Rev. Lett. **97**, 140402 (2006), arXiv:hep-ph/0607118.

[14] D. Feldman, Z. Liu, and P. Nath, Phys. Rev. D **75**, 115001 (2007), arXiv:hep-ph/0702123.

[15] A. Berlin, R. T. D'Agnolo, S. A. R. Ellis, P. Schuster, and N. Toro, Phys. Rev. Lett. **124**, 011801 (2020), arXiv:1908.06982 [hep-ph].

[16] A. Berlin and K. Schutz, (2021), arXiv:2111.01796 [hep-ph].

[17] P. Agrawal *et al.*, Eur. Phys. J. C **81**, 1015 (2021), arXiv:2102.12143 [hep-ph].

[18] K. S. Babu and R. N. Mohapatra, Phys. Rev. Lett. **63**, 938 (1989).

[19] K. S. Babu and R. N. Mohapatra, Phys. Rev. D **41**, 271 (1990).

[20] R. Foot, G. C. Joshi, H. Lew, and R. R. Volkas, Mod. Phys. Lett. A **5**, 2721 (1990).

[21] R. Foot, H. Lew, and R. R. Volkas, J. Phys. G **19**, 361 (1993), [Erratum: J.Phys.G 19, 1067 (1993)], arXiv:hep-ph/9209259.

[22] S. Davidson, B. Campbell, and D. C. Bailey, Phys. Rev. D **43**, 2314 (1991).

[23] K. S. Babu, T. M. Gould, and I. Z. Rothstein, Phys. Lett. B **321**, 140 (1994), arXiv:hep-ph/9310349.

[24] G. Bressi, G. Carugno, F. Della Valle, G. Galeazzi, G. Ruoso, and G. Sartori, Phys. Rev. A **83**, 052101 (2011), arXiv:1102.2766 [physics.atom-ph].

[25] S. N. Gninenko, N. V. Krasnikov, and A. Rubbia, Phys. Rev. D **75**, 075014 (2007), arXiv:hep-ph/0612203.

[26] J.-W. Chen, H.-C. Chi, H.-B. Li, C. P. Liu, L. Singh, H. T. Wong, C.-L. Wu, and C.-P. Wu, Phys. Rev. D **90**, 011301 (2014), arXiv:1405.7168 [hep-ph].

[27] L. Singh *et al.* (TEXONO), Phys. Rev. D **99**, 032009 (2019), arXiv:1808.02719 [hep-ph].

[28] A. N. Khan and W. Rodejohann, Phys. Rev. D **100**, 113003 (2019), arXiv:1907.12444 [hep-ph].

[29] M. Cadeddu, F. Dordei, C. Giunti, Y. F. Li, and Y. Y. Zhang, Phys. Rev. D **101**, 033004 (2020),

arXiv:1908.06045 [hep-ph].

[30] M. Cadeddu, F. Dordei, C. Giunti, Y. F. Li, E. Picciau, and Y. Y. Zhang, Phys. Rev. D **102**, 015030 (2020), arXiv:2005.01645 [hep-ph].

[31] A. N. Khan, Phys. Lett. B **809**, 135782 (2020), arXiv:2006.12887 [hep-ph].

[32] G. Barbiellini and G. Cocconi, Nature **329**, 21 (1987).

[33] G. G. Raffelt, Phys. Rept. **320**, 319 (1999).

[34] S. Davidson, S. Hannestad, and G. Raffelt, JHEP **05**, 003 (2000), arXiv:hep-ph/0001179.

[35] A. Melchiorri, A. Polosa, and A. Strumia, Phys. Lett. B **650**, 416 (2007), arXiv:hep-ph/0703144.

[36] A. I. Studenikin and I. Tokarev, Nucl. Phys. B **884**, 396 (2014), arXiv:1209.3245 [hep-ph].

[37] D. Akimov *et al.* (COHERENT), Science **357**, 1123 (2017), arXiv:1708.01294 [nucl-ex].

[38] D. Akimov *et al.* (COHERENT), (2018), 10.5281/zenodo.1228631, arXiv:1804.09459 [nucl-ex].

[39] D. Z. Freedman, Phys. Rev. **D9**, 1389 (1974).

[40] D. Z. Freedman, D. N. Schramm, and D. L. Tubbs, Ann. Rev. Nucl. Part. Sci. **27**, 167 (1977).

[41] D. L. Tubbs and D. N. Schramm, Astrophys. J. **201**, 467 (1975).

[42] A. Drukier and L. Stodolsky, Phys. Rev. D **30**, 2295 (1984).

[43] J. Barranco, O. G. Miranda, and T. I. Rashba, JHEP **12**, 021 (2005), arXiv:hep-ph/0508299 [hep-ph].

[44] M. Lindner, W. Rodejohann, and X.-J. Xu, JHEP **03**, 097 (2017), arXiv:1612.04150 [hep-ph].

[45] M. Cadeddu, C. Giunti, Y. F. Li, and Y. Y. Zhang, Phys. Rev. Lett. **120**, 072501 (2018), arXiv:1710.02730 [hep-ph].

[46] G. Arcadi, M. Lindner, J. Martins, and F. S. Queiroz, (2019), arXiv:1906.04755 [hep-ph].

[47] D. Aristizabal Sierra, J. Liao, and D. Marfatia, JHEP **06**, 141 (2019), arXiv:1902.07398 [hep-ph].

[48] D. K. Papoulias, T. S. Kosmas, R. Sahu, V. K. B. Kota, and M. Hota, (2019), arXiv:1903.03722 [hep-ph].

[49] A. J. Anderson, J. M. Conrad, E. Figueroa-Feliciano, C. Ignarra, G. Karagiorgi, K. Scholberg, M. H. Shaevitz, and J. Spitz, Phys. Rev. **D86**, 013004 (2012), arXiv:1201.3805 [hep-ph].

[50] P. deNiverville, M. Pospelov, and A. Ritz, Phys. Rev. **D92**, 095005 (2015), arXiv:1505.07805 [hep-ph].

[51] S.-F. Ge and I. M. Shoemaker, JHEP **11**, 066 (2018), arXiv:1710.10889 [hep-ph].

[52] P. Coloma, M. C. Gonzalez-Garcia, M. Maltoni, and T. Schwetz, Phys. Rev. **D96**, 115007 (2017), arXiv:1708.02899 [hep-ph].

[53] M. Bauer, P. Foldenauer, and J. Jaeckel, JHEP **07**, 094 (2018), arXiv:1803.05466 [hep-ph].

[54] J. Billard, J. Johnston, and B. J. Kavanagh, JCAP **1811**, 016 (2018), arXiv:1805.01798 [hep-ph].

[55] P. B. Denton, Y. Farzan, and I. M. Shoemaker, JHEP **07**, 037 (2018), arXiv:1804.03660 [hep-ph].

[56] B. Dutta, S. Liao, S. Sinha, and L. E. Strigari, Phys. Rev. Lett. **123**, 061801 (2019), arXiv:1903.10666 [hep-ph].

[57] D. K. Papoulias and T. S. Kosmas, Phys. Rev. **D97**, 033003 (2018), arXiv:1711.09773 [hep-ph].

[58] A. N. Khan, D. W. McKay, and W. Rodejohann, Phys. Rev. D **104**, 015019 (2021), arXiv:2104.00425 [hep-ph].

[59] O. Tomalak, P. Machado, V. Pandey, and R. Plestid, JHEP **02**, 097 (2021), arXiv:2011.05960 [hep-ph].

[60] D. Akimov *et al.*, (2021), arXiv:2110.07730 [hep-ex].

[61] A. N. Khan, Phys. Lett. B **819**, 136415 (2021), arXiv:2008.10279 [hep-ph].

[62] E. Aprile *et al.* (XENON), Phys. Rev. D **102**, 072004 (2020), arXiv:2006.09721 [hep-ex].

[63] S. Knapen, J. Kozaczuk, and T. Lin, Phys. Rev. Lett. **127**, 081805 (2021), arXiv:2011.09496 [hep-ph].

[64] W. J. Marciano and A. Sirlin, Phys. Rev. D **22**, 2695 (1980), [Erratum: Phys.Rev.D 31, 213 (1985)].

[65] J. Erler and M. J. Ramsey-Musolf, Phys. Rev. **D72**, 073003 (2005), arXiv:hep-ph/0409169 [hep-ph].

[66] P. A. Zyla *et al.* (Particle Data Group), PTEP **2020**, 083C01 (2020).

[67] S. R. Klein and J. Nystrand, Phys. Rev. Lett. **84**, 2330 (2000), arXiv:hep-ph/9909237.

[68] K. Fujikawa and R. Shrock, Phys. Rev. Lett. **45**, 963 (1980).

[69] P. Vogel and J. Engel, Phys. Rev. D **39**, 3378 (1989).

[70] M. Abak and C. Aydin, Nuovo Cim. A **101**, 597 (1989).

[71] W. Grimus and P. Stockinger, Phys. Rev. D **57**, 1762 (1998), arXiv:hep-ph/9708279.

[72] J. Bernabeu, L. G. Cabral-Rosetti, J. Papavassiliou, and J. Vidal, Phys. Rev. **D62**, 113012 (2000), arXiv:hep-ph/0008114 [hep-ph].

[73] J. Bernabeu, J. Papavassiliou, and J. Vidal, Phys. Rev. Lett. **89**, 101802 (2002), [Erratum: Phys. Rev. Lett.89,229902(2002)], arXiv:hep-ph/0206015 [hep-ph].

[74] J. Bernabeu, J. Papavassiliou, and J. Vidal, Nucl. Phys. **B680**, 450 (2004), arXiv:hep-ph/0210055 [hep-ph].

[75] H. Novales-Sanchez, A. Rosado, V. Santiago-Olan, and J. J. Toscano, AIP Conf. Proc. **1540**, 21 (2013).

[76] M. Cadeddu, C. Giunti, K. A. Kouzakov, Y. F. Li, A. I. Studenikin, and Y. Y. Zhang, Phys. Rev. **D98**, 113010 (2018), arXiv:1810.05606 [hep-ph].

[77] A. N. Khan, J. Phys. G **46**, 035005 (2019), arXiv:1709.02930 [hep-ph].

[78] Y. B. Zel'dovich, Soviet Phys. JETP **6**, 1184 (1958).

[79] Y. B. Zel'dovich and A. Perelomov, Zhur. Eksptl'. i Teoret Fiz. **39** (1960).

[80] A. Barroso, F. Boudjema, J. Cole, and N. Dombey, Z. Phys. C **28**, 149 (1985).

[81] M. Abak and C. Aydin, Europhys. Lett. **4**, 881 (1987).

[82] M. J. Musolf and B. R. Holstein, Phys. Rev. D **43**, 2956 (1991).

[83] V. M. Dubovik and V. E. Kuznetsov, Int. J. Mod. Phys. A **13**, 5257 (1998), arXiv:hep-ph/9606258.

[84] A. Rosado, Phys. Rev. **D61**, 013001 (2000).